Improvements in the SOAST Code

Y. Yamauchi, G.L. Kulcinski, C.D. Croessmann

August 1988

UWFDM-767

FUSION TECHNOLOGY INSTITUTE

UNIVERSITY OF WISCONSIN

MADISON WISCONSIN

Improvements in the SOAST Code

Y. Yamauchi, G.L. Kulcinski, C.D. Croessmann

Fusion Technology Institute
University of Wisconsin
1500 Engineering Drive
Madison, WI 53706

http://fti.neep.wisc.edu

August 1988

UWFDM-767

IMPROVEMENTS IN THE SOAST CODE

Y. Yamauchi*, G.L. Kulcinski
Fusion Technology Institute
University of Wisconsin
Madison, Wisconsin 53706

C.D. Croessmann
Fusion Technology Division
Sandia National Laboratories
Albuquerque, New Mexico 87185

August 1988

*On Leave from National Research Institute for Metals, Sengen, Tsukuba 305, Japan

UWFDM-767

1. INTRODUCTION

The control of plasma disruptions in tokamaks is a major issue for future reactors. The survival of reactors after one or a series of disruptions is essential even though it is hoped that most of the instabilities can be eliminated by feedback control [1]. Disruptions can cause damage to a reactor in two ways. One is the impulsive mechanical force generated by electromagnetic induction. This requires appropriate safety margins in mechanical designs. The other is the intensive heat flux deposition onto the first wall by high temperature plasma particles. The survival requires either a breakthrough in first wall design or in materials themselves since carbon components, which are most popular in current devices, can only be guaranteed to operate safely during normal operation.

In order to determine the requirements of first wall materials and components, computer simulations (with appropriate calibration to experiments) have been utilized. SOAST [2], which is a streamlined version of A*THERMAL [3], is one of such computer codes used to simulate a one-dimensional model including surface heat deposition, vaporization at the surface, vapor shielding of the heat flux and heat conduction into substrate. This code has been used in numerous analyses of various materials and conditions and it agrees reasonably well with experiments [2].

However, some improvements can still be made for more accurate simulation. In this report we will describe these improvements with interesting results for a double layered material. The computational algorithms, which are used in SOAST, will not be repeated here in detail as they are discussed in References 2 and 3.

2. SUBROUTINES AND THEIR FUNCTIONS

The SOAST code is written in a extended version of FORTRAN 77, but it can be run on any computer with minor changes due to precompiler, I/O extension and timer subroutines. The flow chart of the SOAST code including present improvements is shown in Fig. 1. The code consists of three major subroutines, i.e., INPUT, FINITE and OUTPUT. These original structures and functions are described as follows.

The subroutine INPUT first reads input data and then, if it is first run, it calls subroutine MESH to make a one-dimensional grid mesh for finite difference calculations. Another option, if the data includes "startup", calls subroutine INITIAL to initialize all variables and flags. If the data includes "stoprun" calls library subroutine EXIT to stop the job.

Subroutine FINITE is the main subroutine used to calculate the heat conduction by a finite difference technique considering external heat deposition onto the surface, vaporization of materials from the surface, melting of substrates and resolidification. It first calls subroutine FLUX to calculate the energy deposition rate by disruption at time t_0, then calls subroutine TPROP to estimate new material data such as thermal conductivity, specific heat and density at the temperature of the previous time step. The subroutine SPTTER is called optionally to estimate the sputtering erosion rate. It then calls subroutine VAPOR to calculate the vaporization rate of the material from the surface. After it calls subroutine COEFFT to carry out the Crank-Nicolson implicit method to get new temperatures at every grid point, it calls subroutine TCHECK to examine all grid zones which are melted, going to be melted, solid, or resolidifying. The algorithms of this phase transition treatment will be described later. After repeating loop c several times, subroutine

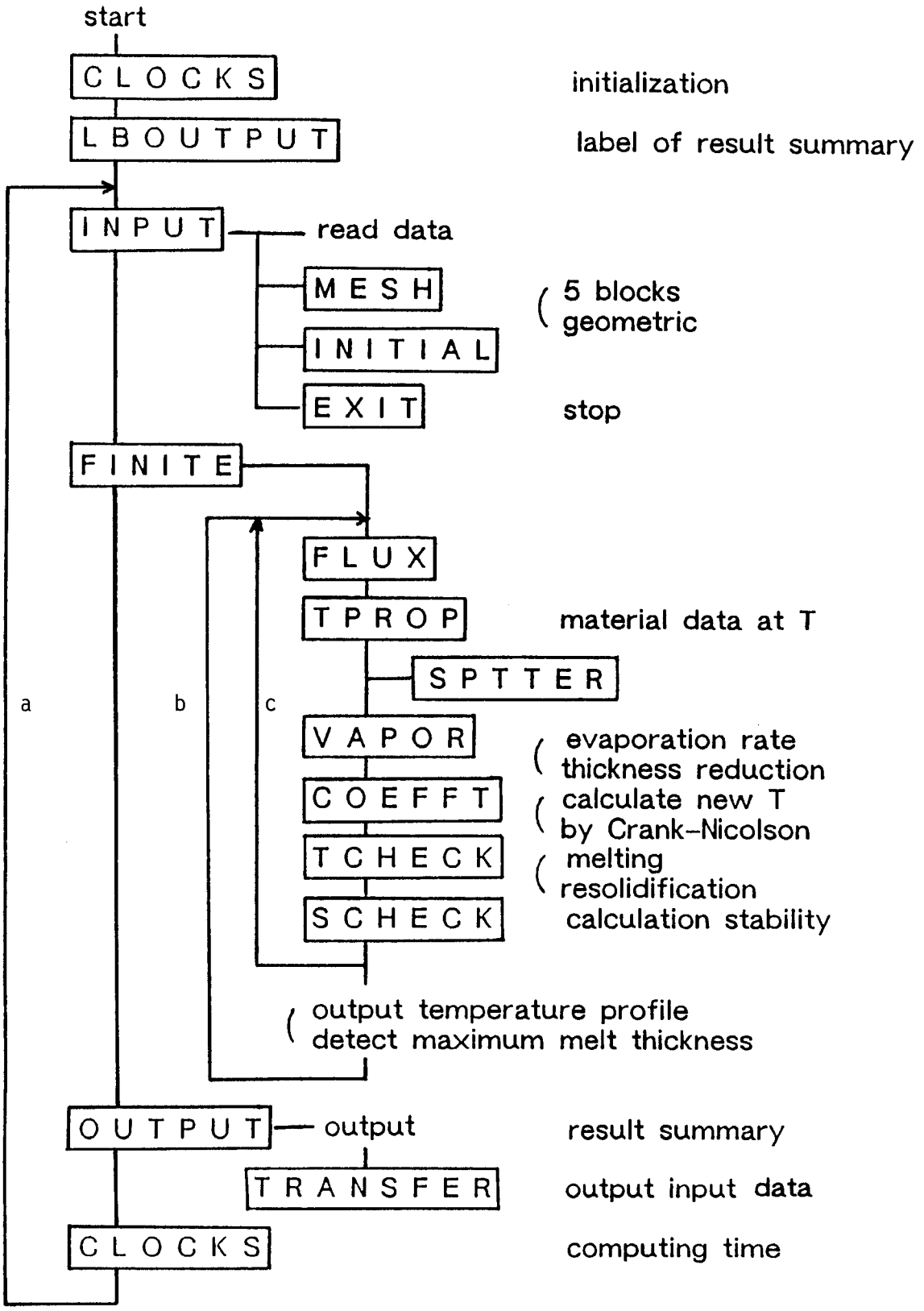

Figure 1. The flow chart of the SOAST code including improvements.

FINITE outputs the temperatures of all grid points and also searches the boundary between the melted and solid zones. Then it repeats loop b for sufficient time periods to complete the work.

The subroutine OUTPUT writes a result summary into the output file which describes the total vaporized thickness, maximum melted zone thickness, etc. It then calls subroutine TRANSFER to output the input data.

The subroutine CLOCK only checks the time for computer charges and outputs it into result summary. SOAST can perform multiple runs going through loop a.

The methods used to simulate melting and resolidification in SOAST are not exact but accurate enough, simple and quite stable. Subroutine TCHECK always checks temperatures of all grid points whether the temperature crosses the melting point or not at each time step. If the temperature exceeds the melting point TCHECK keeps the temperature at the melting point and at the same time estimates the heat corresponding to the artificial temperature reduction and further accumulates it as the latent heat as shown in Fig. 2. After the accumulated latent heat reaches the heat of fusion, subroutine TCHECK changes the flag of the material phase to liquid which causes the code to examine the melting section and to initiate a check of the resolidification. In the case of resolidification, the algorithm is quite similar except for the difference between accumulation and subtraction.

The description above is pertinent to the original SOAST code minus the capability of double layered material simulation which will be discussed in the next section. Hereafter SOAST2 denotes the new modified version of the SOAST code.

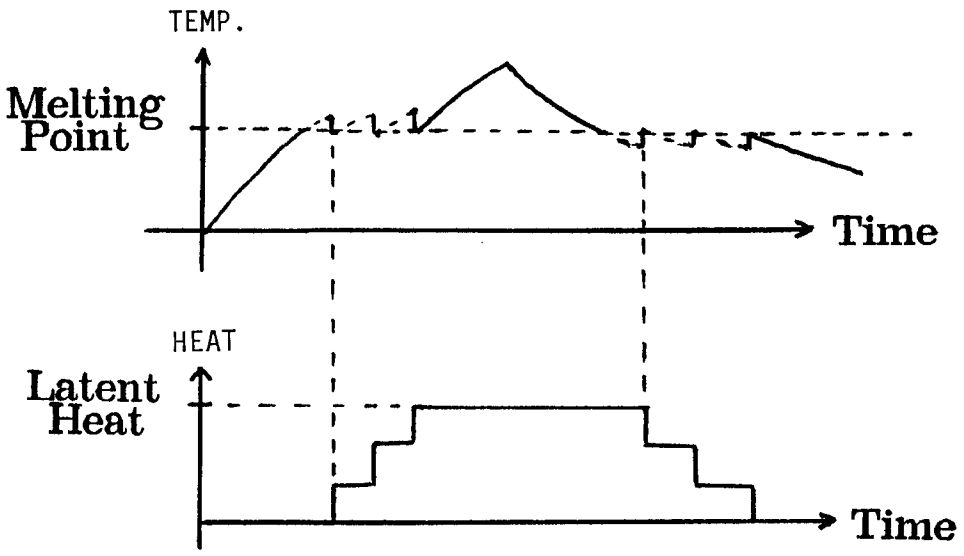

Figure 2. Schematic diagrams of the algorithms to simulate phase transitions between solid and liquid.

3. DOUBLE LAYERED MATERIALS

Coating materials such as carbon, TiC or Mo, have been used to achieve both the suppression of high-Z impurities in plasma and the refractory performance. At present, brazed composites such as W/Cu or C/inconel are emerging as the most capable high heat flux components. The SOAST code is capable of studying those double layered materials. The algorithms adopted in SOAST are useful and quite simple. The first wall components have to be divided into two regions, i.e., coating (depth D) and substrate (deeper than D) as shown in Fig. 3. For double layered structures the relevant subroutines TPROP and TCHECK have the capability to check each depth of every grid point. If z, the distance of a grid point from the surface is greater than D, these subroutines choose the physical quantities of the coated material. In the other case these subroutines choose those of the substrate. The coated thickness D is fixed in SOAST, but this assumption would not be adequate to simulate conditions in which the erosion was large compared to D. In SOAST2 the subroutine VAPOR is modified to reduce the thickness D as the coating material is vaporized. Simple algorithms of double layered material simulation make this improvement easy.

Temperature depth profiles are indispensable in examining the multilayer effect precisely. However, the temperature depth profiles provided by SOAST contain some numerical artifacts which originate from the sudden shifting of mesh sizes. The finite element mesh of SOAST consists of those in 5 different sizes, i.e., finer at the top surface and coarse at the back surface to reduce the computation time. The subroutine MESH of SOAST2 is revised to make the mesh change according to that of a geometric series. This smooth shifting of mesh sizes eliminates graphic "humps" completely and provides us an advantage

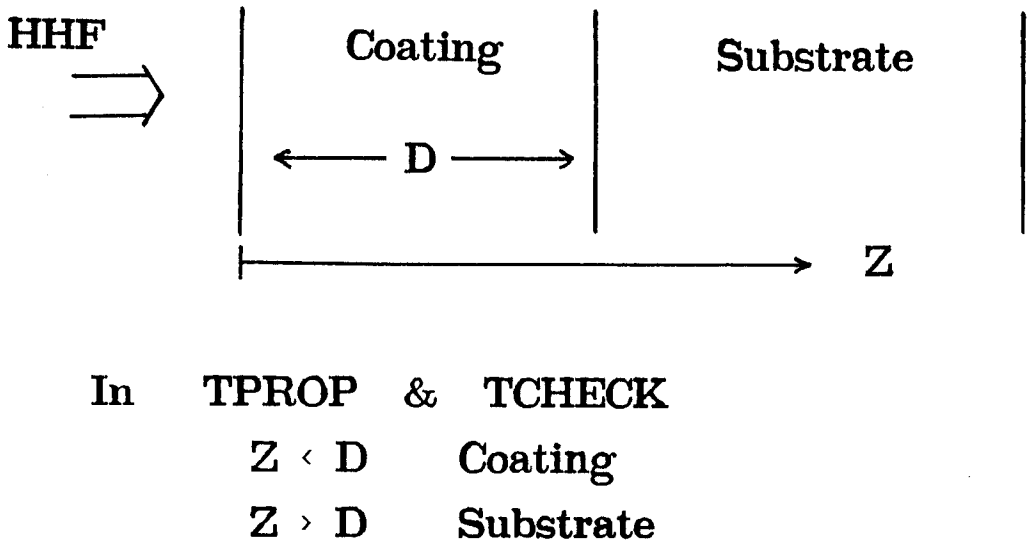

Figure 3. Schematic drawing for the double layered material simulation.

to monitor not only multilayer effects but also physically reasonable behavior of melting and resolidification.

4. HIGH ENERGY DENSITY DEPOSITIONS

High heat flux simulations which include material vaporization from surfaces must be carried out carefully in the case of extremely high energy density deposition. Figure 4 is a deposited energy dependence of maximum melted layer thickness. Somewhat unphysical behavior can be seen in this figure in that while the deposited energy is increased, we would expect the surface temperature to increase also. But the melted thickness actually decreases. The tendency toward saturation in the higher energy density cases can be accepted because of heat removal by the latent heat of intense vaporization. In the calculation of Fig. 4 abnormal temperature oscillations were found above 3 kJ energy deposition by using a dynamic debugging utility. The oscillations can be caused by a too large rate of heat removal by the latent heat of vaporization. The vaporization rate is increased much more drastically at high temperatures. This nature of high nonlinearity leads to oscillatory behavior in the finite element calculation. Once too much heat is removed from the surface by extremely large vaporization rates, then a small vaporization takes place at the next time step due to low surface temperature. After that, a large amount of deposited energy is absorbed and overheating of the surface begins again. The nonlinearity causes not only temperature oscillations but also excess total vaporization. This fact leads to excessive heat removal by the latent heat of vaporization in total and decreases net heat absorbed into the wall which finally decreases the maximum melt layer thickness. Fortunately, this numerical instability was confirmed to be avoidable

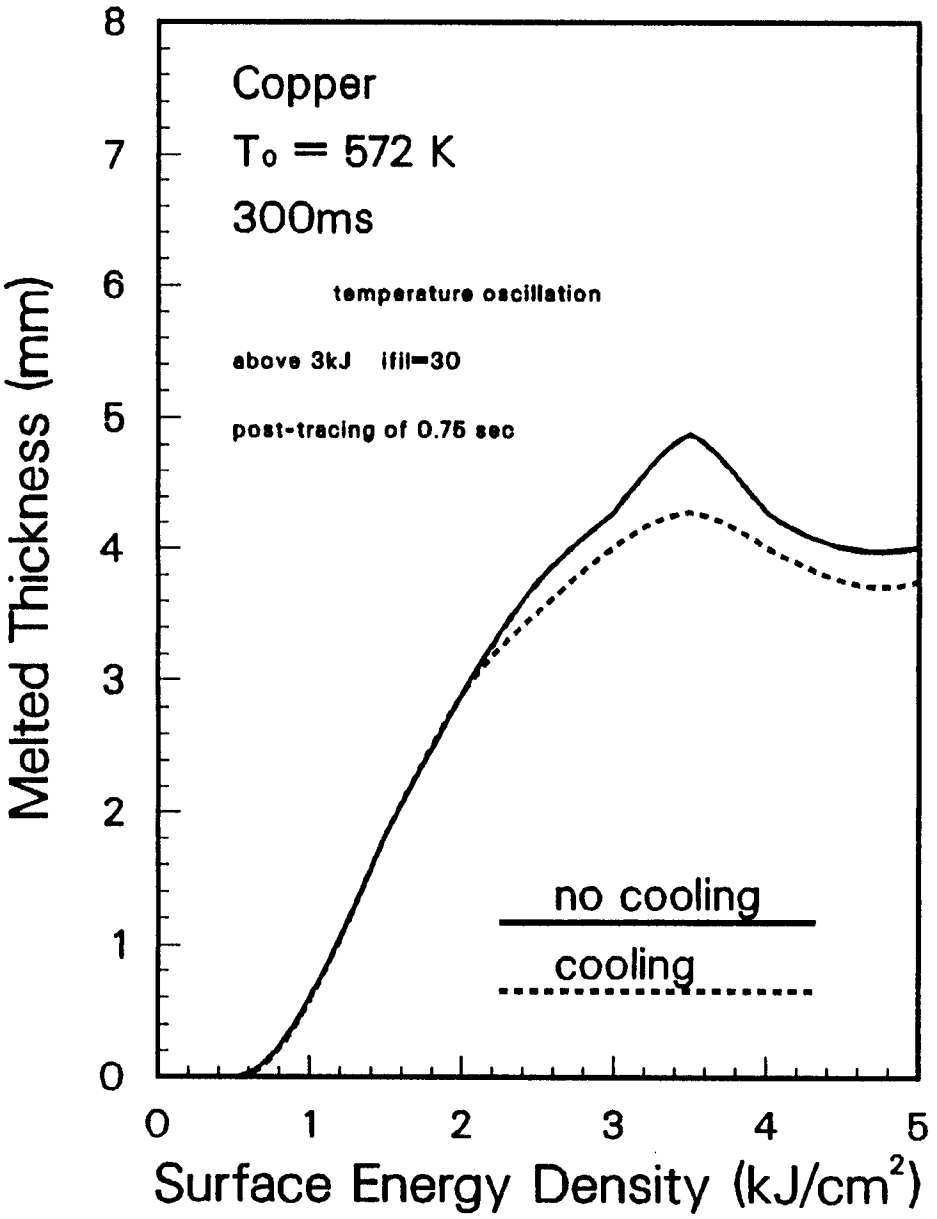

Figure 4. Maximum melted layer thickness versus deposited energy density calculated with the time step of 50 μs and total tracing time of 1.05 s.

by simply setting a fine enough time step. In addition, it was found that a rather long time period is needed to trace the maximum melted layer thickness completely because of a relatively low heat conduction rate.

To monitor these instabilities of the melted layer, the subroutine SCHECK is attached to SOAST2 and the subroutine FINITE is also modified somewhat as shown in Fig. 1. Figure 5 is a plot of an improved result by SOAST2 with the same conditions as Fig. 4 except for the time step and the time period. The curves show the reasonable monotonical increase even in the high energy region.

5. RESULTS ON W/Cu COMPOSITE

From the design study of TIBER II/ITER, a new design of divertor tiles is suggested which is a brazed composite of a tungsten block and a water cooled copper tube to be able to remove the heat deposited during a long time pulse [4]. We examined this composite system from the point of view of disruption rather than from the original quasi-steady condition. Figures 6 and 7 show temperature profiles of the W/Cu composite. Deposited heat flux density is 1 kJ/cm^2 during 10 ms in the case of a relatively thin tungsten layer. In Fig. 6b irregularities can be clearly seen. Due to melting of copper around 1300 K and tungsten at around 3800 K and due to the proximity of the interface at 0.2 mm, the maximum surface temperature in Figure 6a is lower than Fig. 7a. This leads to lower erosion vaporization and could be an advantage of the 0.2 mm tungsten composite. However, of course, the maximum interface temperature in Fig. 6a is much higher than Fig. 7a and this could be a disadvantage.

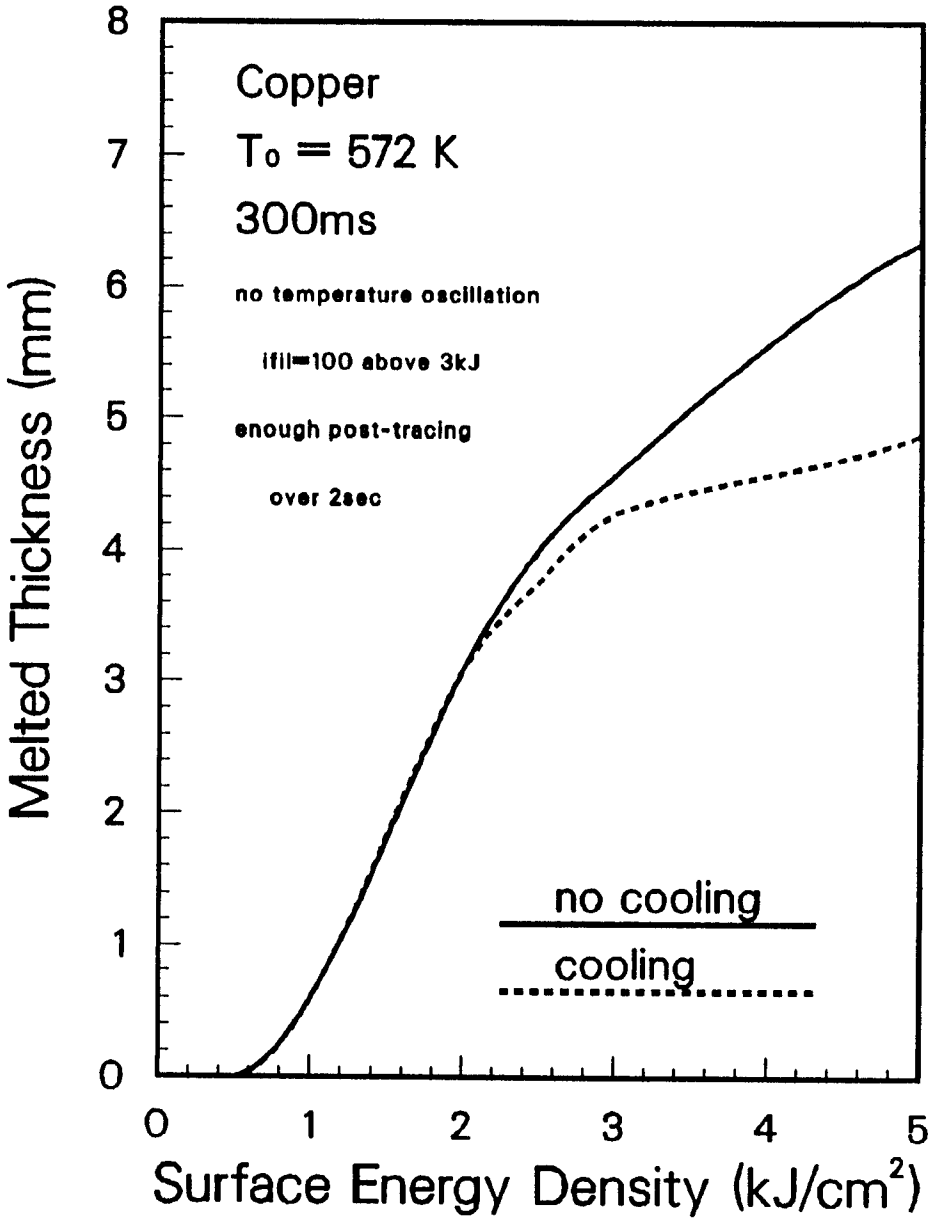

Figure 5. Maximum melted layer thickness versus deposited energy density calculated with the time step of 15 μs and total tracing time over 2 s.

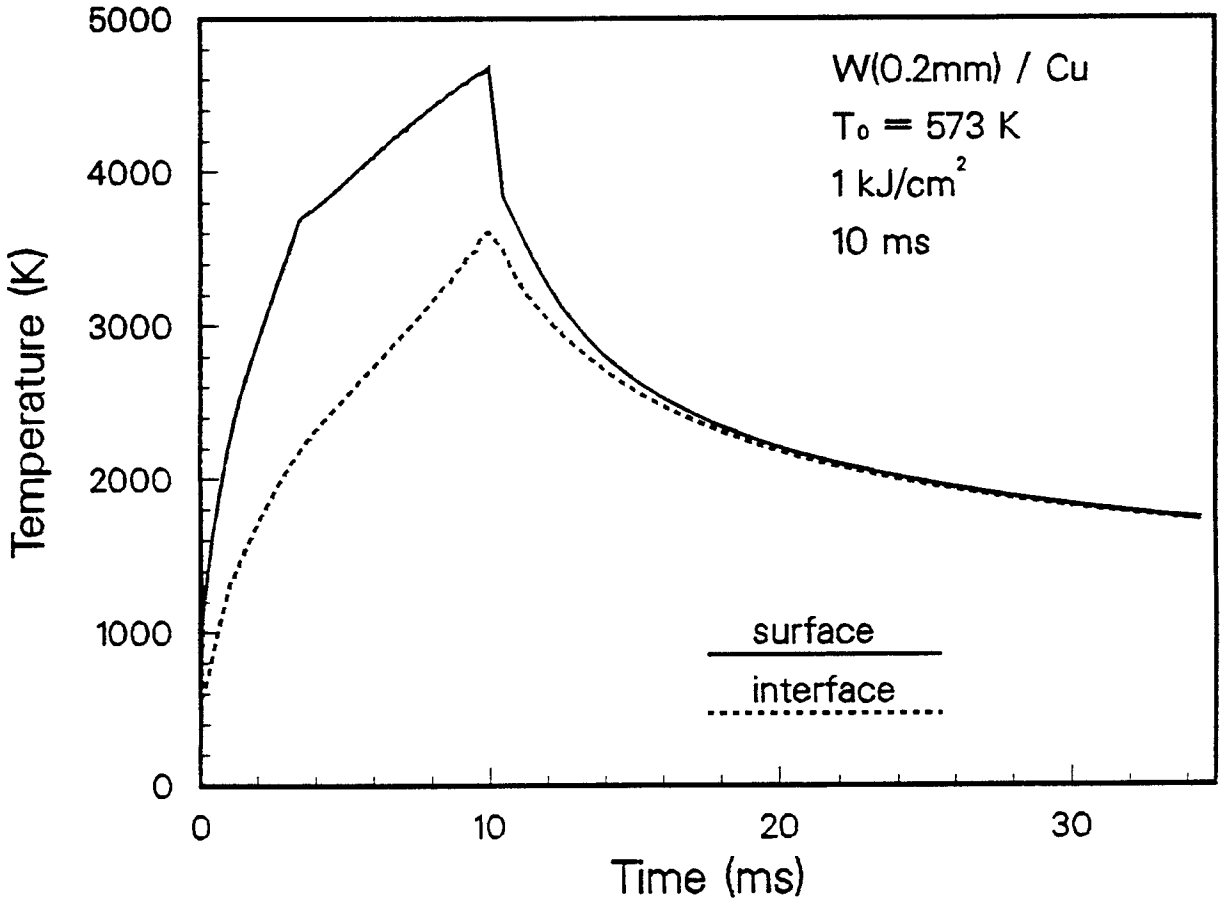

Figure 6a. Surface and interface temperature of 0.2 mm thick tungsten and 12 mm thick copper composite versus time.

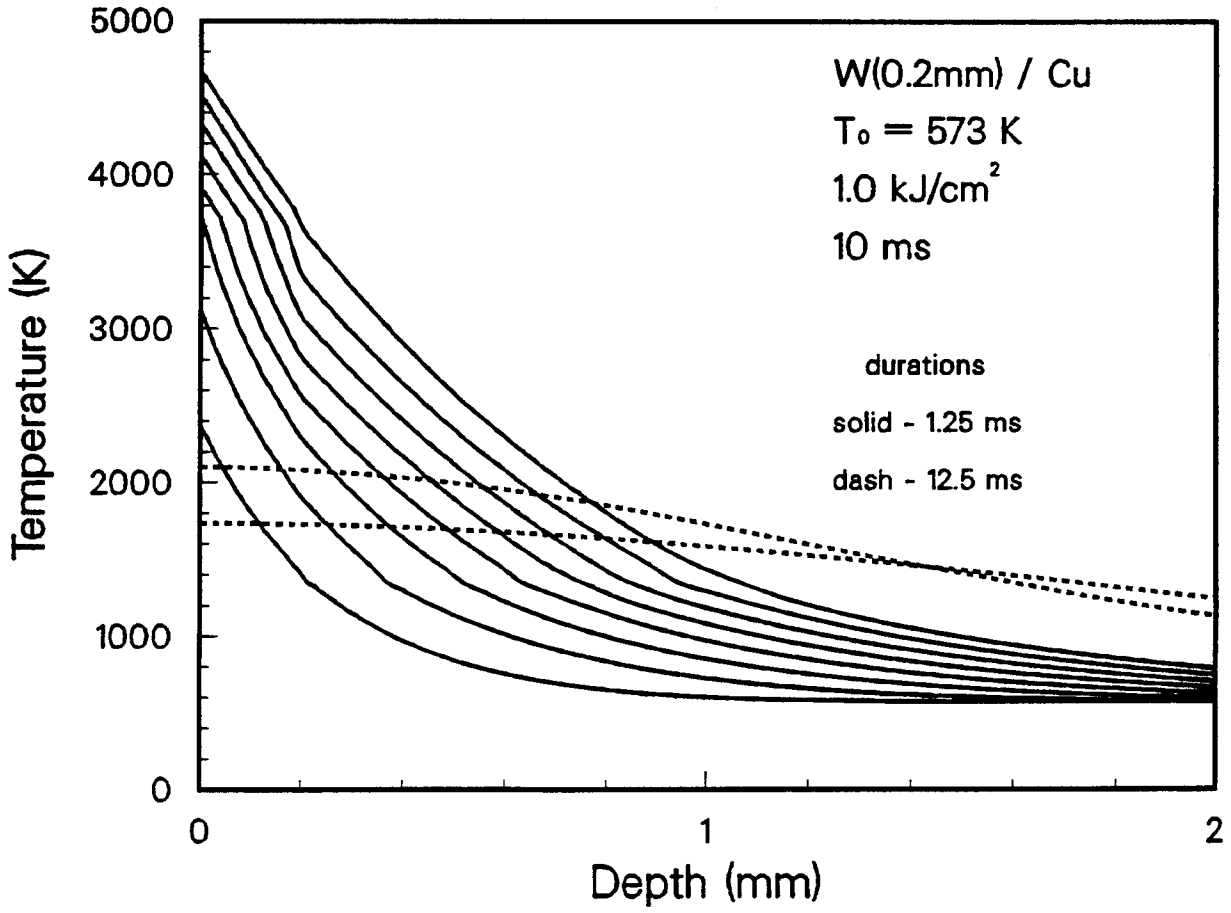

Figure 6b. Temperature depth profiles of same calculation in (a) at several different times.

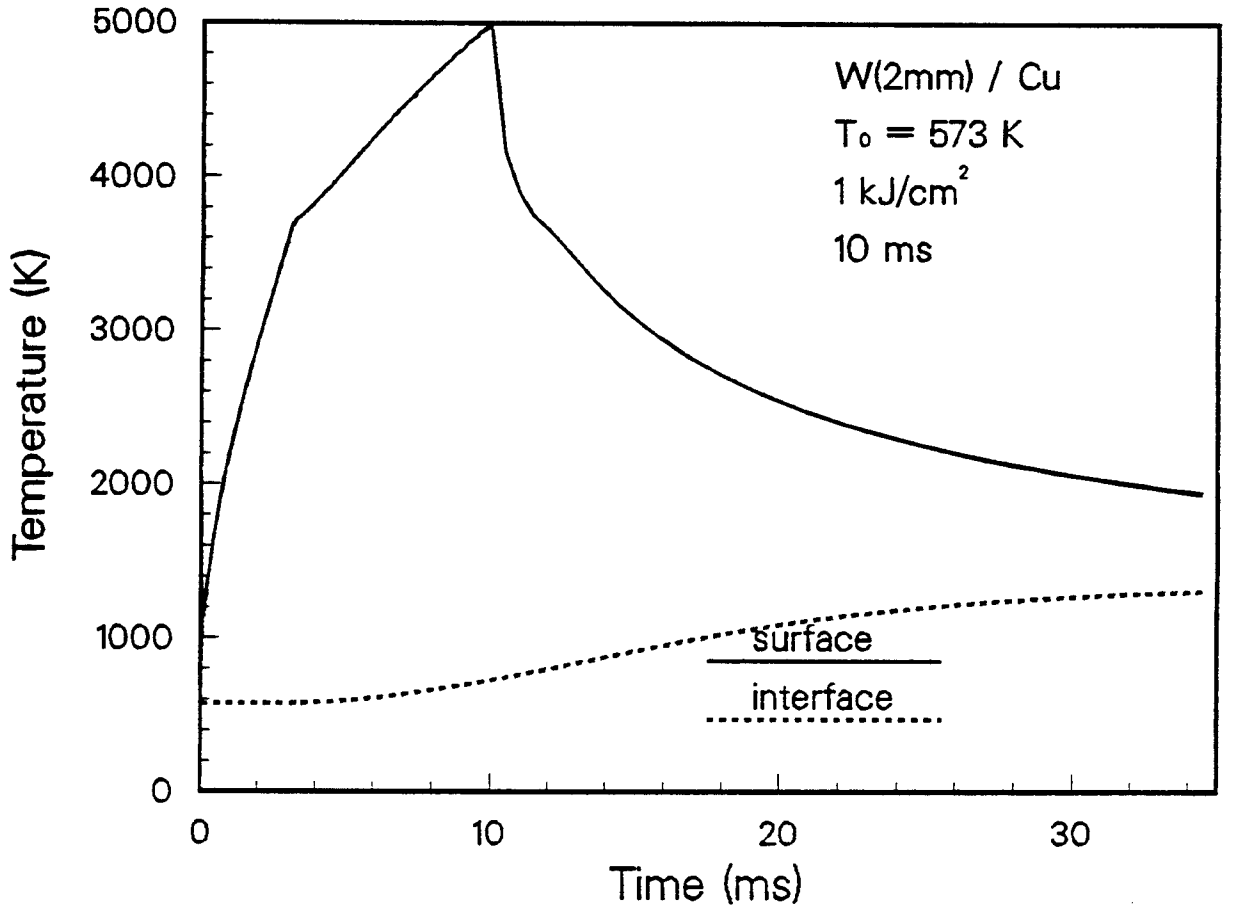

Figure 7a. Surface and interface temperature of 2 mm thick tungsten and 10 mm thick copper composite versus time.

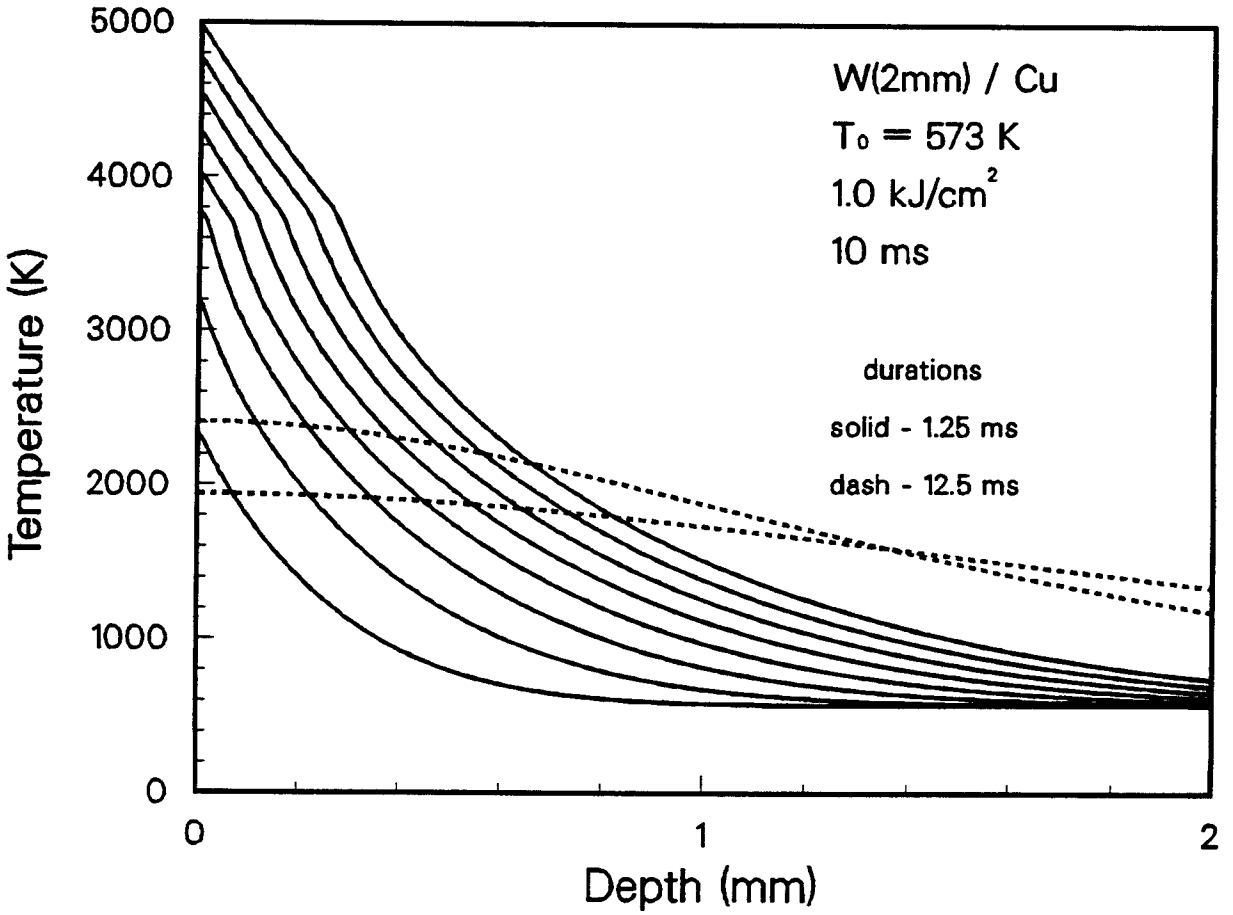

Figure 7b. Temperature depth profiles of same calculation in (a) at several different times.

Summarized vaporized thickness and melted layer thickness data versus the tungsten thickness are shown in Fig. 8 and 9. Both figures indicate that it is possible to reduce the vaporization thickness and melt thickness of tungsten by adopting a thinner tungsten layer. Of course there is a limitation to this reduction due to the loss of sputtered material. On the other hand, from a structural safety point of view, one might adopt the critical thickness from Fig. 9, at which copper does not melt.

In Fig. 10 and 11, data for vaporization thickness over various energy densities and deposition times are summarized. One can see the large differences between the various conditions in copper. As a general rule, the vaporized material is more sensitive to the deposited energy than the deposition time. This is because the deposition time dependency tends to saturate due to the significant amount of heat removal by the latent heat during intense vaporization.

6. CONCLUDING REMARKS

It has been shown that the modification of SOAST to SOAST2 described here provides the following advantages.

- A precise simulation for double layered materials taking into account thinning of the first layer.
- The capability to check temperature profiles in detail for physical consistency.
- An accurate simulation in the regimes of very high energy deposition without calculational instability.

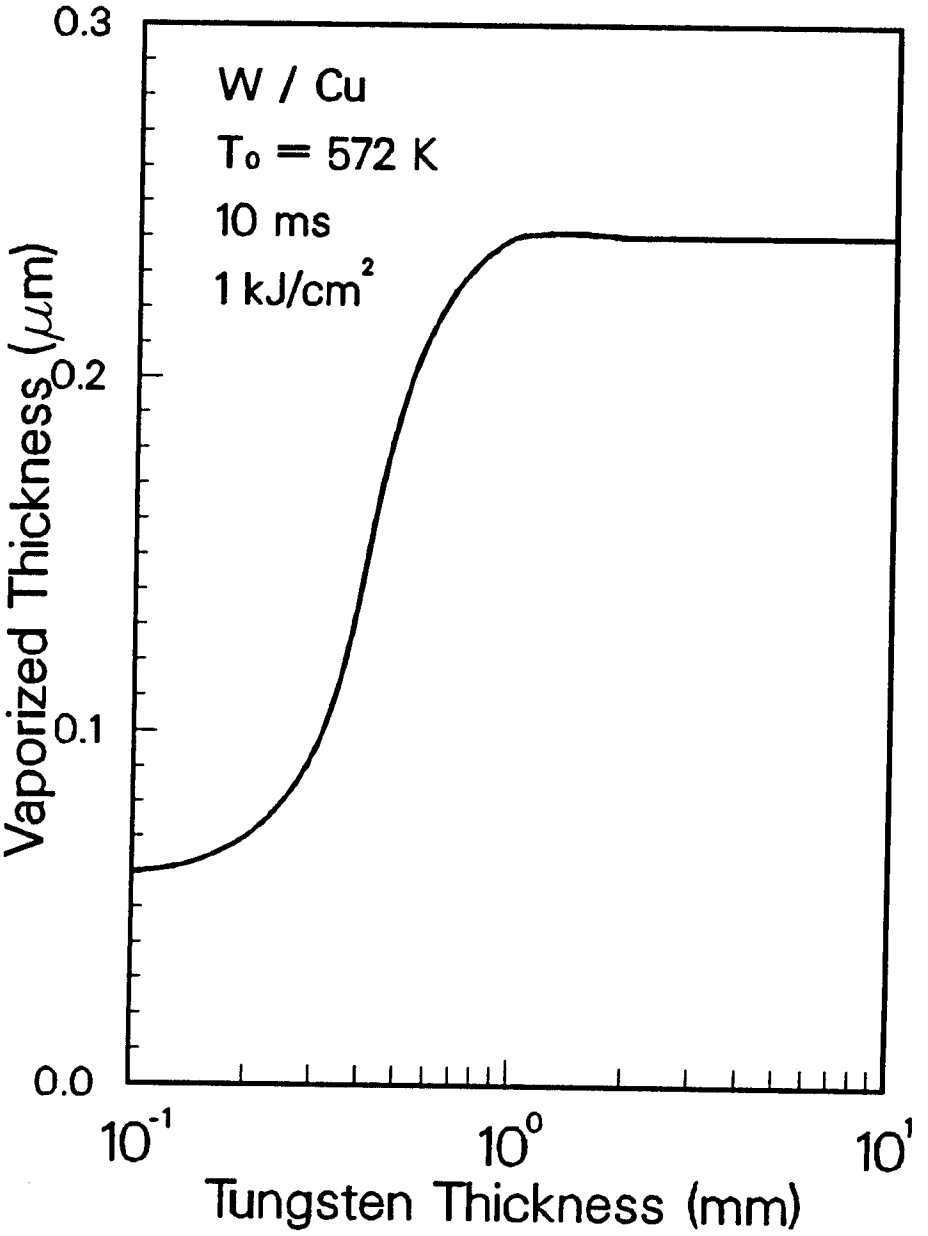

Figure 8. Vaporized thickness of tungsten of W/Cu composite by heat deposition of 1 kJ/cm^2 in 10 ms versus tungsten thickness.

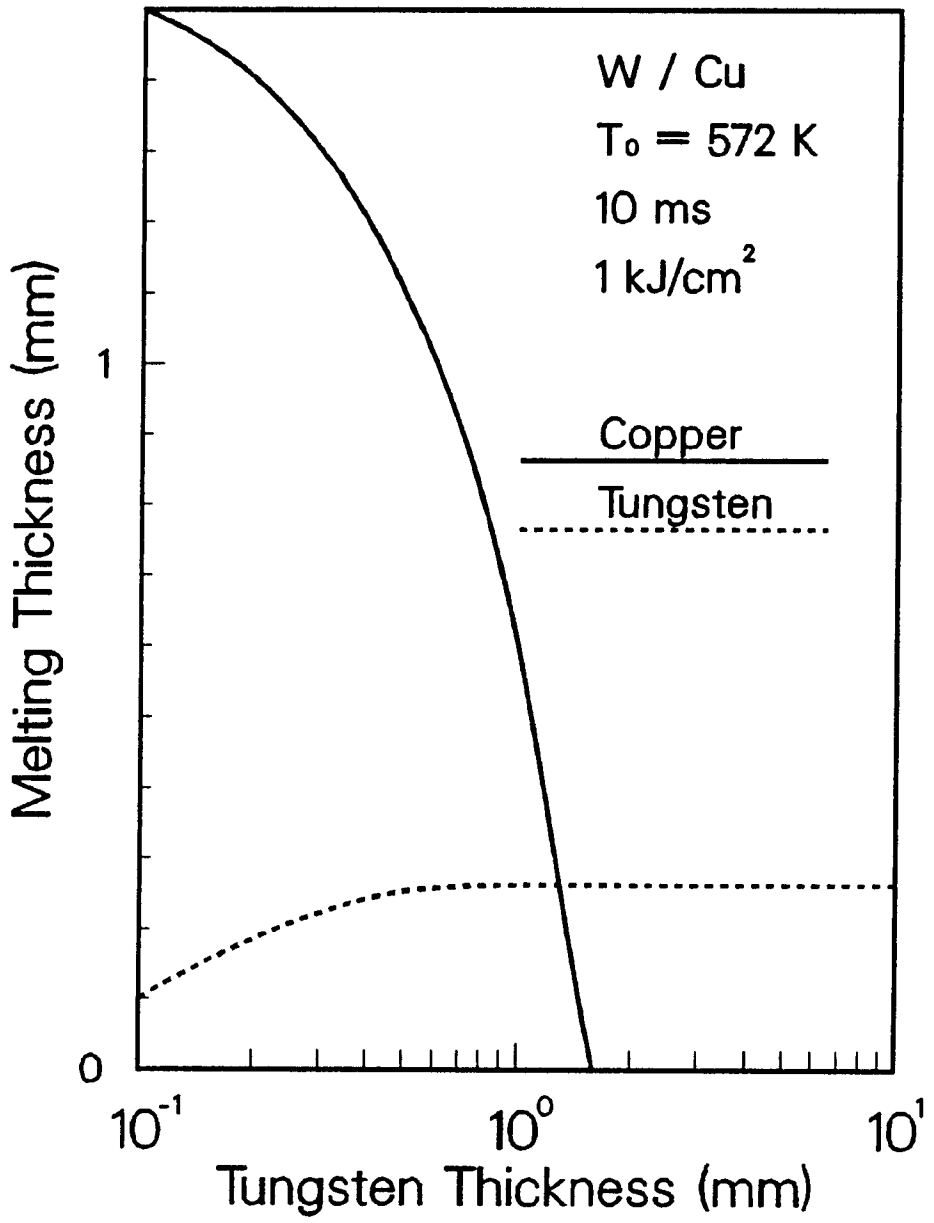

Figure 9. Maximum melted thicknesses of tungsten and copper of W/Cu composite by heat deposition of 1 kJ/cm^2 in 10 ms versus tungsten thickness.

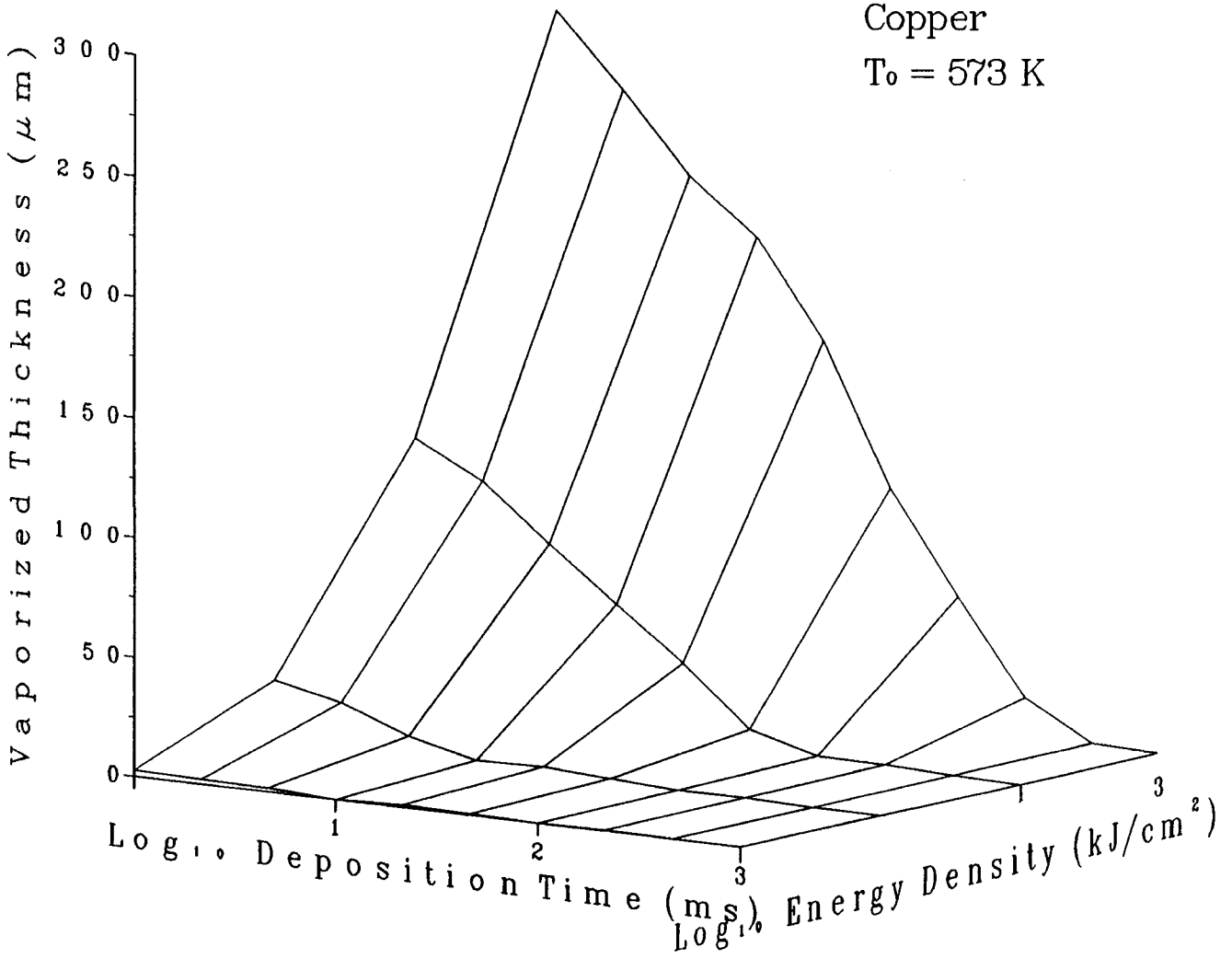

Figure 10. Vaporized thickness of copper by various energy density depositions in different time periods.

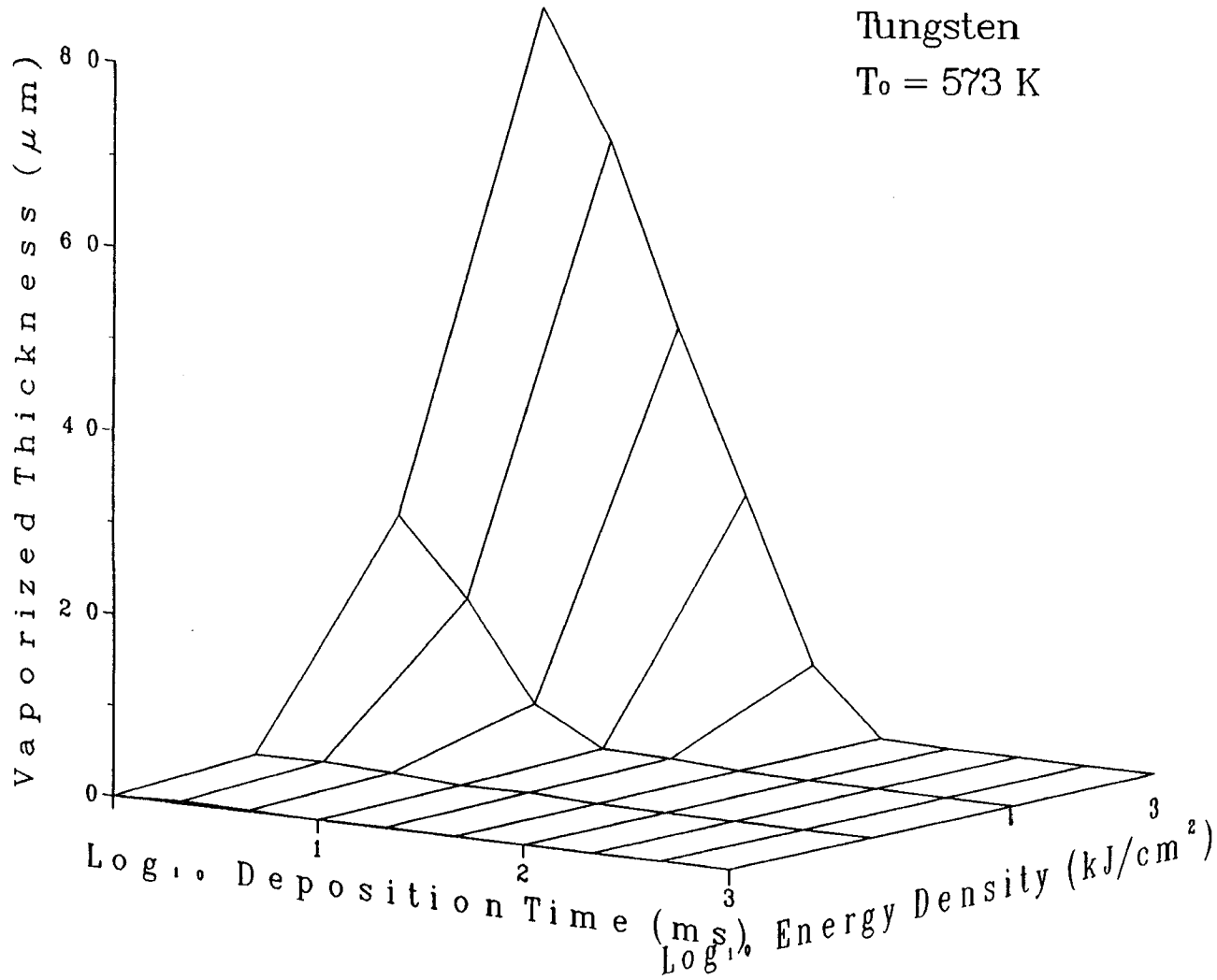

Figure 11. Vaporized thickness of tungsten by various energy density depositions in different time periods.

As to the instability of numerical calculation described in Section 4, a further improvement is still desired. Because subroutine SCHECK only skips the current calculation and jumps to the next one, when it detects the abnormal temperature oscillation, a trial and error procedure is required to get an appropriate value for the time step. An automatic time step control eliminates this trouble. At the time t^{n+2} after the time step $\Delta t^{n+1/2}$, the next time step can be determined from a set of constraints:

$$\Delta t^{n+3/2} = \text{Max}\left[\Delta t_{min}, M_{in}\left(\Delta t_{max}, \frac{K_1\,\Delta t^{n+1/2}}{R_1^{n+1}}, \frac{K_2\,\Delta t^{n+1/2}}{R_2^{n+1}}\right)\right] \qquad (1)$$

where

$$R_1^{n+1} = \left| T_{surf}^{n+1} - T_{surf}^{n} \right| \Big/ T_{surf}^{n+1/2} \qquad (2)$$

$$R_2 = \left| H_{vap}^{n+1} - H_{vap}^{n} \right| \Big/ H_{vap}^{n+1/2} \,. \qquad (3)$$

T_{surf} and H_{vap} are the surface temperature and latent heat rate of vaporization respectively (n+1/2 denotes the mean of n+1 and n+2).

It should be noted that there are other, much more essential, improvements to be added, i.e. vapor shielding model. Comprehensive computer simulations for vapor shielding effects have been published [5,6]. Most of the studies are focused on the plasma physics for reactor designs. Among them the radiation hydrodynamic approach [7] can be adequate to simulate well defined conditions of high heat flux material testing where candidate materials or

components are heated by regulated beams. An appropriate model based on Eulerian coordinates might be capable of simulating the phenomena within a relatively small area during relatively long time periods.

ACKNOWLEDGEMENTS

Computer time was provided by National Magnetic Fusion Energy Computer Center. The 2-D and 3-D graphics programs used herein had been written by Dr. B.B. Glasgow and Mr. S. Han respectively. One of the authors was supported by Atomic Energy Bureau, Science and Technology Agency, Prime Minister's Office, Japan (Y.Y.).

REFERENCES

[1] Panel on Steady State Issues, DOE, Magnetic Fusion Energy Plasma Interactive and High Heat Flux Components (University of California, Los Angeles 1988) Vol. 5, UCLA/PPG-1125.

[2] C.D. Croessmann, Ph.D. Thesis, University of Wisconsin Fusion Technology Institute Report UWFDM-674 (1986).

[3] A.M. Hassanein, Ph.D. Thesis, University of Wisconsin Fusion Technology Institute Report UWFDM-465 (1982).

[4] J.D. Lee, ed., TIBER/ETR Final Design Report (University of California, LLNL 1987) UCID-21150, Vol. 2.

[5] B.J. Merrill, S.C. Jardin and M.C. Carrol, Proceedings of the 10th Symposium of Fusion Engineering, IEEE 83CH1916-6 (1983) 1291.

[6] J.G. Gilligan and D. Hahan, Journal of Nuclear Materials 145-147 (1987) 391.

[7] R.R. Peterson, University of Wisconsin Fusion Technology Institute Report UWFDM-670 (1986).

APPENDIX A

Input, Output Data and Samples of the SOAST2 Code

INPUT DATA:

Paramtr

1) nspace - number of space divisions

2) ntime - number of time steps

3) deltx - space increment at top surface

4) epcil - ratio of geometric series

5) tp - 0.0

6) tau - 0.001

7) alfa - 1.0

8) beta - 0.0

9) isput - 0

10) iflux - switch for vapor shielding option (0-off, 1-on)

11) itype - 0

12) inap - 0

13) npts - number of time steps within disruption time

14) ne - number of time divisions of disruption heat deposition

15) ifil - number of iterations in each time step

16) ifin - number of skipped time steps between temperature outputs

17) iscool - switch for active cooling at bottom surface (0-off, 1-on)

18) iswprfl - switch for temperature output (0-off, 1-on)

19) tamb - initial material temperature (K)

20) stipr - 1.0

21) inc - multiplier for time steps after disruption

Coating

1) range - range of particles being studied in coated material (cm)

2) tmelt - melting temperature of coating material (K)

3) hl - latent heat of fusion (cal/mol)

4) am - atomic mass

5) hvap - heat of vaporization (cal/mol)

6) pzero - vapor pressure is put in by

7) hsub - log 10 (p(atm)) = pzero - hsub/T(k) in low range

8) pz1 - log 10 (p(atm)) = pz1 - hs1/T(K) in high range

9) hz1 -

10) tchg - temperature for changing above range (K)

11-14) dncoatsa, h, c, d - $a + bT + cT^2 + dT^3$ curve fitting coefficients for solid density (g/cm^3) vs. temperature (K)

15-18) dncoatla, b, c, d - liquid density (g/cm^3)

19-22) shcoatsa, b, c, d - specific heat of solid (cal/gK)

23-26) shcoatla, b, c, d - specific heat of liquid (cal/gK)

27-30) tdcoastla, b, c, d - thermal diffusivity of solid (cm^2/s)

35) matcoat - "name of coated material"

36) thick - thickness of coated material (cm)

Substrt

1) tmelt2 - melting temperature of substrate (K)

2) hfus2 - latent heat of fusion of substrate (cal/mol)

3) atomicm - atomic mass

4) matsub - "name of substrate material"

5-8) densubsa, b, c, d - $a + b + CT^2 + dT^3$ curve fitting coefficients for solid density (g/cm^3) versus temperature (K)

9-12) densubla, b, c, d - liquid density (g/cm^3)

13-16) shsubsa, b, c, d - specific heat of solid (cal/gK)

17-20) shsubla, b, c, d - specific heat of liquid (cal/gK)

21-24) tdsubsa, b, c, d - thermal diffusivity of solid (cm^2/s)

25-28) tdsubla, b, c, d - thermal diffusivity of liquid (cm^2/s)

Disrptn

1) drpttime - divided disruption times (s)

2) drptheat - disruption heats in each divisions of disruption time (J/cm^2)

OUTPUT DATA:

Result Summary

1) disrupt.time - total disruption time
2) disrupt.heat - disruption heat at first division
3) evapara.thickne - vaporized thickness of coated material
4) melting coating - melted thickness of coated material
5) melting substra - melted thickness of substrate
6) max.temp surface - maximum temperature at top surface
7) max. temp intrface - maximum temperature at interface
8) in st - detection of calculation instability (0-no, 1-detected)
9) co ol - switch for active cooling at bottom surface (0-off, 1-on)
10) V.S. - switch for vapor shielding option (0-off, 1-on)
11) coating thickne - thickness of coated material
12) substra.thickne - thickness of substrate material
13) unweigh timeused - computer time for each run
14) time execution - start time of each run
15) coat mat. - name of coated material
16) subs mat. - name of substrate material

Temperature Profiles

Temperature depth profiles, time depending temperature profiles at the top surface and the interface can be put into output files, i.e., dpthtmp, surtemp and inttemp respectively which are created automatically.

SAMPLES:

Input Data

```
inwcu
paramtr
   nspace=105     ntime=350     deltx=1.e-4  epcil=1.0673
       tp=0.0       tau=1.e-3    alfa=1.0      beta=0.0     isput=0
    iflux=0       itype=0       ivap=1        npts=200
       ne=1        ifil=30       ifin=25    iswcool=0     iswprfl=0
     tamb=573     stipr=1.0      inc=10
   $
coating
      range=1.6e-4      tmelt=3683.          hl=8430.          am=184.
      pzer0=3.1000       hsub=-34000.      hvap=205000.
        pz1=7.2000        hs1=-42722.      tchg=2500.
   dncoatsa=19.35    dncoatsb=0.0       dncoatsc=0.0       dncoatsd=0.0
   dncoatla=17.600   dncoatlb=0.0000    dncoatlc=0.0       dncoatld=0.0
   shcoatsa=0.0302   shcoatsb=5.63e-6   shcoatsc=2.43e-10  shcoatsd=0.0
   shcoatla=0.0550   shcoatlb=0.0       shcoatlc=0.0       shcoatld=0.0
   tdcoatsa=0.729    tdcoatsb=-1.36e-4  tdcoatsc=-5.87e-9  tdcoatsd=0.0
   tdcoatla=0.440    tdcoatlb=0.0       tdcoatlc=0.0       tdcoatld=0.0
    matcoat="Tungsten" thick=0.1
   $
substrt
    tmelt2=1356.        hfus2=3110.      atomicm2=63.5 matsub="Copper"
   densubsa=8.000    densubsb=0.0        densubsc=0.0       densubsd=0.0
   densubla=9.3700   densublb=-9.44e-4   densublc=0.0       densubld=0.0
    shsubsa=0.085     shsubsb=-2.36e-5    shsubsc=0.0        shsubsd=0.0
    shsubla=0.1220    shsublb=0.0         shsublc=0.0        shsubld=0.0
    tdsubsa=1.245     tdsubsb=-3.38e-4    tdsubsc=0.0        tdsubsd=0.0
    tdsubla=0.322     tdsublb=7.5e-5      tdsublc=0.0        tdsubld=0.0
   $
disrptn
   drpttime= 0.010
   drptheat= 1000.
   $
startup
paramtr
    iswcool=1
   $
disrptn
   drpttime= 0.02
   $
startup
stoprun
```

Output Data Results Summary

```
********* result summary of SOAST ********* 08/20/88
0000500001111151111222225222233333533334444454444555555 555566665666677777577778888858888999959999000005000011111511111
disrupt. disrupt. evapora. melting  melting  max.temp max.temp in co v. coating  substra. unweigh.    time    coat  subs
  time     heat   thickne. coating  substra. surface  intrface st ol s. thickne. thickne. timeused excution mat.  mat.
   ms     J/cm2   micron     mm       mm        K        K      y1 y1 y1    mm        mm        s     hh mm ss
  10.0   1000.0    0.24     0.281    0.710    4997.1   1802.7   0  0  0    1.00     11.16     6.33   14:14:27 Tung  Copp
  10.0   8000.0    0.00     0.001    0.000    3683.0    573.0   1  1  0    1.00     11.16     0.03   14:15:01 Tung  Copp
```